Biocompatible polyvinyl alcohol nanofibers loaded with amoxicillin and salicylic acid to prevent wound infections

Biocompatible Polyvinyl Alcohol Nanofibers loaded with Amoxicillin and Salicylic Acid To Prevent Wound Infections

Ayca Aydin[1,2], Songul Ulag[1,3,7], Ali Sahin[4], Burak Aksu[5], Oguzhan Gunduz[1,6,7], Cem Bulent Ustundag[2,7], Ioana Cristina Marinas[9], Mihaela Georgescu[9], Mariana Carmen Chifiriuc[8,9,10]

[1] Center for Nanotechnology & Biomaterials Application and Research (NBUAM), Marmara University, Istanbul, Turkey;

[2] Department of Bioengineering, Faculty of Chemical and Metallurgical Engineering, Yildiz Technical University, Istanbul, Turkey;

[3] Department of Metallurgical and Materials Engineering, Institute of Pure and Applied Sciences, Marmara University, Istanbul, Turkey;

[4] Genetic and Metabolic Diseases Research and Investigation Center, Marmara University, Istanbul, Turkey;

[5] Department of Medical Microbiology, School of Medicine, Marmara University, Istanbul, Turkey;

[6] Department of Metallurgical and Materials Engineering, Faculty of Technology, Istanbul, Turkey;

[7] Health Biotechnology Joint Research and Application Center of Excellence, 34220 Esenler, Istanbul, Turkey;

[8] Department of Microbiology and Immunology, Faculty of Biology, University of Bucharest, 060101, Bucharest, Romania;

[9] Research Institute of the University of Bucharest (ICUB), 050568, Bucharest, Romania;

[10]Romanian Academy, 050045, Bucharest, Romania.

Address correspondence to Cem Bulent Ustundag, Center for Nanotechnology & Biomaterials Application and Research (NBUAM), Marmara University, Istanbul, Turkey; Health Biotechnology Joint Research and Application Center of Excellence, 34220 Esenler, Istanbul, Turkey. Electronic mail: cbustun@yildiz.edu.tr

Address correspondence to Mariana C. Chifiriuc, Department of Microbiology and Immunology, Faculty of Biology, University of Bucharest, Bucharest, Romania. Electronic mail: carmen.chifiriuc@unibuc.ro

Abstract

Diabetic wounds are one of the most challenging clinical conditions in diabetes, necessitating the development of new treatments to foster healing and prevent microbial contamination. In this study, polyvinyl alcohol (PVA) was used as a matrix polymer, and amoxicillin (AMX) and salicylic acid (SA) were selected as bioactive compounds with antimicrobial (with AMX) and anti-inflammatory action (with SA) to obtain innovative drug-loaded electrospun nanofiber patches for the management of diabetic wounds. Scanning electron microscopy (SEM) images revealed the uniform and beadless structure of the nanofiber patches. Mechanical tests indicated that AMX minimally increased the tensile strength, while SA significantly reduced it. The patches demonstrated effective antibacterial activity against both gram-positive (Staphylococcus aureus) and gram-negative (Escherichia coli) strains. The potential of these patches in the development of novel wound dressings is highlighted by the excellent biocompatibility with fibroblast cells maintained for up to 7 days.

Keywords: antibiotic; wound dressing; biocompatibility; antimicrobial activity, drug delivery

1. Introduction

Wound refers to the deterioration of tissue integrity due to various diseases or external factors and the inability of living tissue to maintain its structure and function [1]. Diabetes is a prevalent chronic disease caused by a deficiency or inefficiency of the hormone insulin, leading to high blood sugar levels [2]. The wound healing process is delayed in diabetic patients due to the weakening of the body's natural resistance and immune system, impaired blood flow and tissue oxygenation, and the occurrence of wound infections. The process of healing diabetic wounds is challenging and prolonged [3]. According to the estimates of the International Diabetes Federation, the number of diabetic patients will increase to 643 million in 2030 and 783 million in 2045 [4]. The number of diabetic wound cases is expected to follow this

trend; therefore, there is a need to develop effective treatment systems that will contribute to the successful healing of diabetic wounds [5].

It makes it possible to develop new systems and devices through tailor-made properties of matter for various applications in physics, chemistry and biology [6]. It is expected that nanotechnology will solve many biomedical problems, including treating burns and wounds, repairing tissues and organs, and treating various illnesses [7].

The aim of this study is to tackle the challenge of chronic wound management by creating innovative electrospun nanofibre patches using PVA as a matrix polymer. These patches will be loaded with AMX to achieve an antimicrobial effect and SA will be chosen for its anti-inflammatory activity. The goal of delivering drugs through polymer-based nanofibres is to increase the surface area of carriers and enhance the dissolution rate in the required region.

Nanofibers belong to a specific category of nanomaterials with structures and properties that resemble those of natural biological tissues. Their porous nature offers advantages for the healing of tissues [8 - 10]. Their high surface area to volume ratio makes them advantageous for use as dressings. As a result, their use provides a high likelihood of interacting with the biological targets and better penetration, leading to increased adhesion of cells, proteins, and drugs to the wound area.

There are many techniques for producing nanofibers, such as drawing, template synthesis, phase separation, fibrillation, melt-blowing, rotary jet spinning, and electrospinning [11, 12]. The electrospinning method has been used in this study for the fabrication of nano-sized structures. This method enables the combination of different natural or synthetic polymers [13, 14].

Nanoparticles have the functions of carrying active drug release, protecting, maintaining, and providing low drug dosage [15]. By using these functions of nano sizes, it is aimed to load the drug on the nanofiber surface and to support the wound healing process.

When treating wounds and injuries, administering drugs locally to the wound is a faster method of preventing potential infections. Recent studies on antibiotics have shown that excessive use of antibiotics may disrupt body functions and lead to possible side effects. The direct loading of AMX into the wound dressing is designed to avoid the potential side effects of antibiotics, to provide direct protection to the wound and to prevent infection, thereby speeding up the wound healing process.

A number of studies on the dressing of diabetic wounds with nanofibres can be found in the literature. For instance, Cam et al. conducted a study on nanofibrous scaffolds loaded with antidiabetic agents while Samadian et al. conducted a study on nanofiber dressings designed for diabetic foot ulcers. Both studies showed positive results in the development of diabetic wounds [15, 16].

The healing of wounds in diabetic patients is much more difficult due to the weakened defense system of the patients, and the care of the wounds is very important. For this reason, a synergistic effect with both antimicrobial and anti-inflammatory properties is aimed by using AMX and SA together. Thanks to the structural properties of nanofibers, the surfaces obtained will support the proliferation of cells and tissue regeneration by healing.

We have selected PVA as a matrix material in this study, which is a synthetic, hydrophilic, biodegradable, biocompatible, and environmentally friendly polymer, harboring high tensile strength, flex resistance, heat sealing, and moisture permeability [17, 18]. In addition, anticoagulants, commonly known as blood thinners, prevent clots from forming and the growth of clots in blood vessels. It is the most well-known anticoagulant of SA. The compound is a monohydroxybenzoic acid with lipophilic properties and a crystalline structure. It dissolves in water, displays analgesic and anti-inflammatory properties, and shows minimal interaction with other drugs [19, 20]. Another essential feature of wound dressings is to protect the wound against infections, which could evolve into severe clinical forms because of the weakened immune system of diabetic patients. To achieve this, we have incorporated the non-toxic penicillin antibiotic AMX into our patches [21]. The electrospinning method was used to create nanoscale fibres,

which can be used as wound dressings. The aim of these nanofibers formed a structure similar to the extracellular matrix (ECM) and created a porous structure for cell placement, migration, and nutrient and oxygen exchange.

2. Materials and Methods

2.1. Materials

PVA (molecular weight = 89000–98000, hydrolysis degree 99%+) was provided by Sigma Aldrich (USA). AMX (96%) was bought from Acros Organics, and SA was provided by Abdi Ibrahim Pharmaceuticals. Tween 80 and Glutaraldehyde (25% solution in water) were purchased from Merck KGaA, Darmstadt, Germany.

2.2. Preparation and characterisation of the solutions

In the first step, 13 weight percent PVA was dissolved in 20 mL of distilled water at 80 degrees Celsius and 300 revolutions per minute using a magnetic stirrer. Once complete dissolution had been achieved, the solution was cooled down to room temperature. Functional surfaces were obtained by adding 20 mg of SA ($C_7H_6O_3$) and 20 mg of AMX ($C_{16}H_{19}N_3O_5S$) into the 13wt.% PVA solution, which was then mixed on the magnetic stirrer until the drugs had dissolved. Tween 80 was added for surface tension reduction and for the production of beadless nanofibres, which were the result of the addition of Tween 80 to the PVA solution.

The physical properties of the prepared solutions were determined by measuring their density, electrical conductivity, surface tension, and viscosity values. Electrical conductivity was detected using the Cond 3110 SET 1 WTW (Germany), the surface tension was measured with the tensiometer Sigma 703D Attention (Germany), and viscosity values were measured with the DV-E Brookfield Ametek (USA) device.

2.3. Fabrication of drug-loaded patches with the electrospinning method

The electrospinning process comprises three main components: the syringe pump system (supply unit), power supply and collector. In the electrospinning process, it is essential to optimise the flow rate, voltage and distance between the collector and the needle. A laboratory-scale electrospinning machine (Inovenso, Istanbul, Turkey) was used to produce drug-loaded nanofibres. During electrospinning (as shown in Figure 1), we utilized a syringe pump (NE-300, New Era Pump Inc., USA), a single brass needle (1.63 mm diameter) and a power supply. Polymer solutions were prepared and inserted into 10 mL syringes. After that, we adjusted the flow rate and voltage values to 2 mL/h and 28 kV, respectively. We removed the greaseproof paper from the collector after production was completed. As a final step, crosslinking was performed with a crosslinker that links the polymer chains together and provides the formation of a three-dimensional network structure. Glutaraldehyde (GA), which is very effective in stabilising biomaterials and is therefore frequently used, was used as the crosslinking agent for this process. It was used to crosslink the nanofiber patches as a vapour. The patches were placed in the desiccator and kept at 40°C for two hours and then, after cross-linking, left to dry overnight at room temperature.

2.4. Physico-chemical characterisation of the nanofiber patches

The functional groups of components and bond structures were determined by FTIR (Jasco FT/IR-4700) analysis. The transmission mode was adjusted between 4000 cm^{-1} and 450 cm^{-1}. The study was performed at room temperature (23 ^{o}C).

Thermal transition points were analysed for all patches using differential scanning calorimetry (DSC). The temperature range was set between 25°C and 300°C for each patch, with a selected heating rate of 10°C per minute.

The scanning electron microscope (SEM) was used to examine the surface and cross-sectional structures of the nanofiber patches. The patches were coated with gold and then analyzed for morphology using SEM (EVO LS 10, ZEISS).

In the drug release test, firstly, the linear calibration curves of the drugs were determined by measuring the absorbance values of 5 different concentrations of drugs (0.2, 0.4, 0.6, 0.8, and 1 µg mL^{-1}). Release studies were started after determining the characteristic curve and specific wavelength of the drugs. The nanofiber patches loaded with 5 mg AMX and SA were prepared and placed in eppendorf tubes containing 1 mL of phosphate-buffered saline (PBS, pH: 7.4) solution. The sample tubes were incubated in a thermal shaker at 37°C and 300 rpm. Measurements were taken at 15, 30, and 60 min time intervals with UV-Visible Spectrophotometer, and samples were refreshed with PBS after each measure.

The mechanical properties of the nanofiber patches were examined using a uniaxial tensile testing device (Shimadzu Corporation, EZ-LX, Kyoto, Japan). Before the test, the patches were cut to dimensions of 5 cm in length and 1 cm in width. The thickness values of the patches were measured using a digital micrometer (Mitutoyo, USA). The test parameters were set to a test speed and load cell of 5 mm/min and 5 kN, respectively.

2.5. Biological evaluation of the nanofiber patches

The viability of L929 fibroblast cells (CCL-1; ATCC, Rockville, Md., USA) on nanofiber patches was quantitatively determined by the MTT test (4×10^4 cells per well) for 1, 3, and 7 days. After incubation (37°C, 5% CO_2), the culture medium was discarded, and the patches were washed three times with PBS solution. A volume of 90 µl fresh medium and 10 µl MTT solution (5 mg/mL in PBS solution) were added into the 96 well-plate and incubated at 37°C, in a 5% CO_2 atmosphere for 3 hours. Following this, the samples were transferred to clean plates. 200 µl of DMSO was added to dissolve the formazan crystals and the resulting suspension was incubated for 1 hour. Finally, the measurement of the absorbance values was conducted at 540 nm with a microplate reader.

Cell attachment and proliferation on the nanofiber patches were visualised using fluorescence microscopy. The nanofiber patches were collected 1, 3, and 7 days after culture, and washed thrice with PBS solution.

The cells were fixed on or within the materials using 4% paraformaldehyde for 30 minutes, stained using DAPI solution, and then stored in the darkroom for 10 minutes.

The growth medium was removed from the plate for the SEM analysis, and all patches were fixed with 4% glutaraldehyde. Then the patches were dehydrated with diluted ethanol (70%) and dried at room temperature. Prior to the SEM analysis, the dried patches were coated with Au for a period of 60 seconds at a voltage of 10 kV.

The antibacterial activity of the drug-loaded nanofiber patches was tested against the gram-positive *Staphylococcus aureus* (ATCC 29212) and the gram-negative *Escherichia coli* (ATCC 25922) strains. Before the test, the bacterial strains were cultured overnight to get fresh cultures from standardised bacterial suspensions with 0.5. The MacFarland density was determined. Bacterial suspensions were inoculated onto Mueller-Hinton agar plates using an automated plate inoculator. Prior to the test, 5 mm diameter round nanofiber patches were acquired and sterilised under UV light for one hour. A paper filter disk impregnated with 2 µg AMX was used as control, and then the disks were cultured at 37 °C for 18 h. The zones of growth inhibition were measured subsequent to the experiment.

3. Results

First of all, the concentration, viscosity, conductivity and surface tension of the solutions were investigated. Accordingly, the average densities were found 1.038, 1.087, 1.052, and 1.048 g/cm^3; electrical conductivities were found 706.0, 646.0, 631.7, and 609.3 µS/cm; surface tensions were found 35.86, 35.38, 37.74, and 37.36 mN/m; viscosities were found 9760, 7030, 7875, and 7223 mPa.s for crosslinked 13wt.% PVA, 13wt.% PVA+AMX, 13wt.% PVA+SA, and 13wt.% PVA+AMX+SA solutions, respectively (Table 1).

The FTIR analysis was performed to examine the chemical interactions of the obtained matrices, and Figure 2 showed that spectrums of crosslinked 13wt.% PVA (A, a), AMX (A, b), SA (A, c), crosslinked

13wt.% PVA+AMX (A, d), crosslinked 13wt.% PVA+SA (A, e), and crosslinked 13wt.% PVA+AMX+SA (A, f) matrices. The FTIR analysis investigated the chemical interactions between the drugs and the polymer matrix. Figure 2A presents the FTIR spectra. The peaks observed at ~3279.4 cm^{-1} (O-H stretching), ~2905.2 cm^{-1} (CH_2 asymmetric stretching), ~1417.4 cm^{-1} (C=O carbonyl stretching), ~1323.9 cm^{-1} (C–H bending vibration of CH_2), ~1140.7 cm^{-1} (C–H deformation vibration), ~1086.7 cm^{-1} (C–O stretching of acetyl groups), and ~832.1 cm^{-1} (C-C stretching) detected for crosslinked 13wt.% PVA (Figure 2 (A, a) [22, 23]. Figure 2A (b, c) showed the FTIR spectrums of the pure AMX and SA, respectively. The main peaks for AMX were detected at 1774.4 cm^{-1}, 1685.7 cm^{-1}, 1577.7 cm^{-1}, 1485.1 cm^{-1}, and 1249.8 cm^{-1}. SA had main peaks at 1652 cm^{-1}, 1483 cm^{-1}, 1444 cm^{-1}, 1296 cm^{-1}, and 669 cm^{-1} [24]. Figure 2 A (d, e, f) showed the FTIR spectrums of the crosslinked 13wt.% PVA+AMX, crosslinked 13wt.% PVA+SA, and crosslinked 13wt.% PVA+AMX+SA nanofiber patches and these peaks were almost the same with the crosslinked 13wt.% PVA indicated that drugs were homogeneously distributed in the PVA matrix.

Figure 2B showed DSC thermographs that give information about the amount of energy changing with the temperature investigated of pure drugs, and Figure 2C showed DSC thermographs of crosslinked 13wt.% PVA (C, a), crosslinked 13wt.% PVA+AMX (C, b), crosslinked 13wt.% PVA+SA (C, c), and crosslinked 13wt.% PVA+AMX+SA (C, d) matrices. The glass transition temperatures (T_g) of the pure drugs were found at 100 °C and 142 °C for AMX and SA, respectively. The T_g values of the nanofibers were found at 122 °C, 210 °C, 205 °C, and 207 °C for crosslinked 13wt.% PVA, 13wt.% PVA+AMX, 13 wt.% PVA+SA and 13 wt.% PVA+AMX+SA, respectively.

SEM was utilized for visualization of the produced nanofibers and measurement of their diameters was conducted. The analysis was performed prior to crosslinking (Figure 3), and later repeated after crosslinking (Figure 4) to evaluate the impact of crosslinking on both the morphology and the diameter of the fibers. The average nanofiber diameters of 13wt.% PVA (a), 13wt.% PVA+AMX (b), 13wt.% PVA+SA

(c) 13wt.% PVA+AMX+SA (d) surfaces before crosslinking were 0.35 μm, 0.39 μm, 0.49 μm, 0.48 μm; after crosslinking were 5.05 μm, 4.87 μm, 5.41 μm, 4.95 μm, respectively.

Drug release profiles of AMX and SA drug loaded 13wt.% PVA nanofiber matrices were evaluated by UV-Visible Spectrophotometer (Figure 5). Calibration curves of AMX and SA were obtained (Figure 5 (a, b)), absorbance graphs were created (Figure 5 (c, d)), and cumulative drug releases from nanofiber surfaces were examined (Figure 5 (e, f)). It was observed that the drugs were released within one hour.

Table 2 presents the tensile strength and strain at break values of nanofibers, which were measured using a uniaxial tensile testing device. Based on the results, the 13wt.% PVA had 4.31 ± 0.22 MPa tensile strength value and 34.03 ± 9.55% strain at break value. By the addition of AMX into the 13wt.% PVA, it was obtained that tensile strength value increased to 16.64 ± 2.12 MPa and elongation value increased to the value of 51.58 ± 6.57 %. On the other hand, the tensile strength value decreased to the value of 12.91 ± 1.54 MPa and elongation percentage increased to the 58.89 ± 3.25% with the addition of SA. The 13wt.% PVA+AMX+SA had the 17.48 ± 3.27 MPa tensile strength and 57.29 ± 18.02% elongation values.

Figure 6a demonstrates the cytocompatibility with MTT, indicating that the crosslinked 13wt.% PVA resulted in a cell viability of approximately 65% on day 1, and this ratio decreased to approximately 40% on days 3 and 7. These ratios were approximately 65% on day 1, 75% on day 3, and 95% on day 7. For the crosslinked 13wt.% PVA+AMX matrix, it was observed that it was approximately 60% on the 1st day, approximately 50% on the 3rd day, and approximately 55% on the 7th day. The main matrix with crosslinked 13wt.% PVA+AMX+SA content showed approximately 105% on the 1st day, approximately 100% on the 3rd day and approximately 145% on the 7th day. Figure 6b shows images of cells on nanofibre patches taken with a fluorescence microscope, while SEM images (Figure 7) were used to observe cell growth on nanofibre matrices.

As seen in Table 3, *E.coli* (ATCC 25922) strain showed 0 mm inhibition diameter on all nanofiber surfaces. *S. aureus* (ATCC 29213) strain showed an inhibition zone of 12 mm with crosslinked 13wt.% PVA+AMX

and 6 mm with crosslinked 13wt.% PVA+AMX+SA; did not show an inhibition zone for crosslinked 13wt.% PVA and 13wt.% PVA+SA nanofibers.

4. Discussion

The physical properties of the solutions depend on concentration, viscosity, conductivity, and surface tension; therefore in mixed solutions, when changing one parameter, other parameters can be affected [20, 21]. Table 1 shows that the density and surface tension values did not change significantly when drugs were added to the 13 wt% PVA solution. Only a slight decrease in surface tension was observed with the addition of AMX. An increase in surface tension was observed with the addition of SA. Adding AMX and SA together preserved the increase in surface tension caused by SA. The addition of SA had a greater effect on reducing the electrical conductivity value of the pure PVA solution compared to the addition of AMX. Combining AMX and SA resulted in a synergistic effect that reduced the value. Despite the decrease in electrical conductivity due to drug addition, the value remained adequate for the formation of nanofibers. The addition of AMX and SA decreased the viscosity values, with AMX having a greater impact. The addition of SA alone to the solution resulted in a lower reduction in viscosity compared to the addition of AMX. The addition of AMX considerably altered the viscosity, but its combination with SA reduced this value once again.

The FTIR spectrums that were performed to examine the chemical interactions between the drugs and the polymer matrix were given in Figure 2A. The main peaks for 13wt.% PVA observed at 3279.4 cm^{-1}, 2905.2 cm^{-1} , 1417.4 cm^{-1}, and 1086.7 cm^{-1} (Figure 2 (A, a)). The main peaks for AMX (Figure 2 (A, b)) were detected at 1774.4 cm^{-1}, 1485.1 cm^{-1}, and 1249.8 cm^{-1}. These peaks were additionally detected for 13wt.% PVA+AMX and 13wt.% PVA+AMX+SA (Figure 2A (d, f)) crosslinked nanofibers. The SA (Figure 2 (A, c)) had main peaks at 1652 cm^{-1}, 1296 cm^{-1}, and 669 cm^{-1} [25]. The Figure 2A (f) showed the FTIR

spectrum of the crosslinked 13wt.% PVA+AMX+SA nanofiber patch and these peaks were almost the same with the crosslinked 13wt.% PVA.

PVA is a synthetic semi-crystalline polymer that thermally degrades over 200 ^{o}C and then crystallises from a molten state very rapidly, preventing the inconvenience of obtaining a completely amorphous polymer [26]. The DSC results of pure drugs and nanofiber patches were shown in Figure 2B and Figure 2C, respectively. The glass transition temperatures (T_g) of the pure drugs were found at 100 ^{o}C and 142 °C for AMX and SA, respectively, and also pure PVA nanofiber was found at 122 ^{o}C. The incorporation of drugs raised the glass transition temperature (Tg) significantly above 200 ^{o}C. Furthermore, there was no noticeable variation between the impact of AMX and SA on the Tg value. Although there were some shifts in the peaks, the distinctive peaks of the pure drugs were not prominently observed on the nanofiber patches.

The Figure 3 showed the non-crosslinked 13wt.% PVA, 13wt.% PVA+AMX, 13wt.% PVA+SA, and 13wt.% PVA+AMX+SA nanofiber patches, respectively. All patches exhibited homogeneous and beadless structures. The distributions of the diameters of the patches are shown in Figure 3. The average diameters were found 350±0.16 nm, 390±0.17 nm, 490±0.16 nm, and 484±0.18 nm for 13wt.% PVA, 13wt.% PVA+AMX, 13wt.% PVA+SA, and 13wt.% PVA+AMX+SA, respectively. These results showed that drug addition increased the thickness of the fiber diameters. Another study showed similar results after adding SA into the 13wt.% PVA [27]. This may be a result of the adhesive structure of the SA. However, AMX addition did not result in a significant increase in the diameter of the nanofibers. Owing to the fact that PVA dissolves swiftly in water, crosslinking is essential for maintaining its consistency. As shown in Figure 4, no significant change or deterioration occurred in the morphologies of the nanofibers after cross-linking. Nevertheless, an increase in the diameter of the fibres was observed. The average diameters, after crosslinking, were found 5.05±1.33, 4.87±1.26, 5.41±1.22, and 4.95±1.53 μm for crosslinked 13wt.% PVA, 13wt.% PVA+AMX, 13wt.%PVA+SA, and 13wt.% PVA+AMX+SA nanofibers, respectively.

The drug release behaviours of the AMX and SA from the crosslinked 13wt.% PVA nanofiber patches were observed separately. Figures 5a and 5b presented the calibration curve of the AMX and SA, respectively, and the Figure 5c and 5d displayed the absorbance graphs of the AMX and SA which were obtained at 230 nm and 208 nm, respectively. The cumulative release graph of AMX from the nanofiber patches is shown in Figure 5e. It indicates that the drugs were completely released within one hour. Figure 5f shows the exact release behaviour for SA. According to previous studies [18, 28], PVA's water-soluble nature leads to rapid drug release. Increasing PVA concentration leads to rapid drug release. To achieve sustained drug release, necessary for chronic wounds, PVA must be effectively crosslinked with either glutaraldehyde or UV. In this study, PVA was used, resulting in the drugs being released in a burst manner. Both drugs showed burst release behaviour. This accomplished the goal of PVA degrading rapidly and releasing the drug for wound healing applications.

The flexibility and strength of the nanofibers are also essential features for wound dressings. The tensile strength and elongation at break (%) values of all the nanofiber patches were given in Table 2. PVA is 100% water-soluble and has high tensile strength, high flexural resistance, good heat sealing, and good moisture permeability [29]. Because of its many advantages, this polymer was chosen. As seen in Table 2, AMX addition into the nanofiber patches increased the tensile strength and elongation at break values, making the nanofibers more durable and flexible. Similar to AMX, SA also increased tensile strength and elongation at break values. However, SA addition decreased the tensile strength value from 16.64 ± 2.12 to 12.91 ± 1.54 MPa, although it increased the elongation at break more than AMX. Adding SA resulted in reduced mechanical properties compared to AMX. SA may reduced the strength by causing a weakening in the interactions between the polymer chains. It also increased the average fiber diameter, as seen in Figure 3. In the study of Pant et al., they observed that by adding SA into the PU, the mechanical properties increased, and the highest strength was found for 10% SA addition. The tensile strength and elongation values (17.48 ± 3.27 MPa and 57.29 ± 18.02 %, respectively) suggested that the nanofibers containing

both AMX and SA have enhanced features, probably due to a good interactions of AMX and SA both between them and with PVA matrix.

Biocompatibility is a critical feature for supporting wound healing structures. The nanofiber surface should not be cytotoxic and should simultaneously support cell adhesion and migration to the appropriate region and their local proliferation [30]. The cytocompatibility of the obtained patches were evaluated by the MTT assay, and the results were shown in Figure 6a. The viability of the cells on the crosslinked 13wt.% PVA nanofiber decreased from day 1 to 7, similar to the crosslinked 13wt.% PVA+SA. The viability of the cells cultured on the crosslinked 13wt% PVA+AMX nanofibers increased towards the seventh day. The viability increased by 10% on the first day and then showed a slight drop on the third day, followed by a 50% on the seventh day. In addition, it has been noticed that the crosslinked 13wt.%PVA+AMX+SA provided higher viability compared to the control group.

The MTT results were confirmed via fluorescence microscopy examination. The distribution of DAPI-stained cells on the nanofiber patches was depicted in Figure 6b. Despite the decrease in cell density on day 3, it recovered and exceeded the initial level by day 7. The cell density on the AMX loaded nanofiber patch after 7 days of culture was higher than the density of cells after 1 day of culture.

The morphology of the cells grown on nanofiber patches is depicted in Figure 7, after 1, 3 and 7 days of culture. It could be noticed that the dendritic fibroblast structure is more well preserved in the case of cells adhered to the crosslinked 13wt.% PVA+AMX and crosslinked 13wt.% PVA+SA nanofibers. In the study of B. Pant et al., SA was added to the solution of the Polyurethane (PU) at different concentrations (5%, 10%, and 15%). According to their results, the cell proliferation was higher for SA added PU nanofibers than PU nanofibers after 1, 3, and 6 days of incubation. At the end of the 6^{th} day, the viability of the cells reached the highest level [28]. In our study, after 7 days of incubation, cells grown on the AMX and SA loaded patches showed much higher viability than crosslinked 13wt.% PVA nanofiber.

The drug-loaded nanofiber patches were evaluated for their antimicrobial activity against strains of S. aureus and E. coli. A summary of the bacterial growth inhibition zones of the patches and the control of the antibiotics is shown in Table 3. The results showed that the crosslinked 13wt.% PVA+AMX and 13wt.% PVA+AMX+SA patches showed antibacterial activity against *S. aureus*, as revealed by the growth inhibition zone diameter of 12 and 6 mm, but not against *E. coli*. Thus, the obtained could prevent wound contamination with gram-positive bacteria, which is an important result, taking into account that *S. aureus* is a frequent contaminant of the skin and external surfaces, often in the etiology of wound infections. The antibacterial activity of Core-shell silk/PVA nanofibers was studied by N. Ojah et al. They showed that the addition of AMX resulted in antibacterial activity against S. aureus and E. coli [31]. B. Pant et al. conducted a study where they fabricated SA/PU composite nanofibers. They discovered that the PU surface by itself did not have any antibacterial effect. Instead, surfaces with varying concentrations of SA were found to be effective against both S. aureus and E. coli. According to [28], the antibacterial activity of the surfaces increased with increasing SA concentration.

5. Conclusions

This paper reports the fabrication and biological properties of AMX and SA loaded PVA nanofibers designed for chronic, diabetic wound management. The main reason for using AMX and SA together on the wound dressing surface is that it is desired to have both antimicrobial and anti-inflammatory properties on the surface. The reason for this is that the wound dressing both prevents the healing in the wound area from being negatively affected by harmful microorganisms and reduces pain and inflammation in the area. Therefore, a wound dressing with multiple functions has been acquired. The SEM images showed that the uniform, smooth, and beadless structures were obtained with electrospinning technique. The FTIR results indicate that drugs were homogeneously distributed into the crosslinked 13 wt.% PVA. According to the drug release profiles, AMX and SA are released completely after one hour. The patches loaded with AMX and SA showed antibacterial activity against S. aureus. The materials were not found to be cytotoxic

and they supported fibroblast cell proliferation, which can stimulate wound closure. Collectively, these results indicate that drug-loaded cross-linked 13% w/w PVA nanofibres have potential for use in the development of innovative wound care products.

Ethical Statement

No animal or human studies were carried out by the authors for this article; therefore, no ethical approval for this particular study is needed.

Availability of Data and Materials

All data generated or analysed during this study are included in this published article.

Data Availability Statement

The data that support the findings of this study are available upon reasonable request from the authors.

Consent for Publication

This paper reflects the views of the authors and should not be construed to represent the FDA's views or policies.

Conflict of Interest

The authors have no conflicts of interest.

Acknowledgements

This study was supported financially by the Scientific and Technological Research Council of Turkey (TUBITAK), 1139B411901020 project.

I.C.M., M.G.and M.C.C. acknowldge the support of the grant of the Romanian National Authority for Scientific Research, CNCS – UEFISCDI, project PN-III-P2-2.1-PED-2021-2193 (594PED/2022).

ORCID

Ayca Aydin: https://orcid.org/0009-0003-1942-4065

Songul Ulag: https://orcid.org/0000-0001-8215-1504

Ali Sahin: https://orcid.org/0000-0001-5594-1551

Oguzhan Gunduz: https://orcid.org/0000-0002-9427-7574

Cem Bulent Ustundag: https://orcid.org/0000-0002-4439-0878

Ioana Cristina Marinas: https://orcid.org/0000-0002-7342-5398

Mihaela Georgescu: https://orcid.org/0000-0002-0115-2693

Mariana Carmen Chifiriuc: https://orcid.org/0000-0001-6098-1857

References

1. Croitoru, A.-M.; Karaçelebi, Y.; Saatcioglu, E.; Altan, E.; Ulag, S.; Aydoğan, H.K.; Sahin, A.; Motelica, L.; Oprea, O.; Tihauan, B.-M.; et al. Electrically Triggered Drug Delivery from Novel Electrospun Poly(Lactic Acid)/Graphene Oxide/Quercetin Fibrous Scaffolds for Wound Dressing Applications. *Pharmaceutics* **2021**, *13*, 957, doi:10.3390/pharmaceutics13070957.

2. Hussein, M.A.M.; Su, S.; Ulag, S.; Woźniak, A.; Grinholc, M.; Erdemir, G.; Erdem Kuruca, S.; Gunduz, O.; Muhammed, M.; El-Sherbiny, I.M.; et al. Development and In Vitro Evaluation of Biocompatible PLA-Based Trilayer Nanofibrous Membranes for the Delivery of Nanoceria: A Novel Approach for Diabetic Wound Healing. *Polymers (Basel)* **2021**, *13*, 3630, doi:10.3390/polym13213630.

3. Spampinato, S.F.; Caruso, G.I.; de Pasquale, R.; Sortino, M.A.; Merlo, S. The Treatment of Impaired Wound Healing in Diabetes: Looking among Old Drugs. *Pharmaceuticals* **2020**, *13*, 60, doi:10.3390/ph13040060.

4. Magliano, D.J.; Boyko, E.J. *International Diabetes Federation. IDF Diabetes Atlas*; 10th ed.; IDF DIABETES ATLAS: Brussels, Belgium, 2021;

5. Ren, X.; Han, Y.; Wang, J.; Jiang, Y.; Yi, Z.; Xu, H.; Ke, Q. An Aligned Porous Electrospun Fibrous Membrane with Controlled Drug Delivery – An Efficient Strategy to Accelerate Diabetic Wound Healing with Improved Angiogenesis. *Acta Biomater* **2018**, *70*, 140–153, doi: 10.1016/j.actbio.2018.02.010.

6. Sozer, N.; Kokini, J.L. Nanotechnology and Its Applications in the Food Sector. *Trends Biotechnol* **2009**, *27*, 82–89, doi: 10.1016/j.tibtech.2008.10.010.

7. Dhivya, S.; Padma, V.V.; Santhini, E. Wound Dressings – a Review. *Biomedicine (Taipei)* **2015**, *5*, 22, doi:10.7603/s40681-015-0022-9.

8. Christgau, M.; Caffesse, R.G.; Schmalz, G.; D'Souza, R.N. Extracellular Matrix Expression and Periodontal Wound-Healing Dynamics Following Guided Tissue Regeneration Therapy in Canine Furcation Defects. *J Clin Periodontol* **2007**, *34*, 691–708, doi:10.1111/j.1600-051X.2007.01097.x.

9. Liu, X.; Xu, H.; Zhang, M.; Yu, D.-G. Electrospun Medicated Nanofibers for Wound Healing: Review. *Membranes (Basel)* **2021**, *11*, 770, doi:10.3390/membranes11100770.

10. Valenta, C.; Auner, B.G. The Use of Polymers for Dermal and Transdermal Delivery. *European Journal of Pharmaceutics and Biopharmaceutics* **2004**, *58*, 279–289, doi: 10.1016/j.ejpb.2004.02.017.

11. Leung, V.; Ko, F. Biomedical Applications of Nanofibers. *Polym Adv Technol* **2011**, *22*, 350–365, doi:10.1002/pat.1813.

12. Mirbagheri, M.; Mohebbi-kalhori, D.; Jirofti, N. Evaluation of Mechanical Properties and Medical Applications of Polycaprolactone Small Diameter Artificial Blood Vessels. *International Journal of Basic Science in Medicine* **2017**, *2*, 58–70, doi:10.15171/ijbsm.2017.12.

13. Li, W.; Tuan, R.S. Fabrication and Application of Nanofibrous Scaffolds in Tissue Engineering. *Curr Protoc Cell Biol* **2009**, *42*, doi:10.1002/0471143030.cb2502s42.

14. Yeum, J.H.; Yang, S.B.; Sabina, Y. Fabrication of Highly Aligned Poly(Vinyl Alcohol) Nanofibers and Its Yarn by Electrospinning. In *Electrospinning - Material, Techniques, and Biomedical Applications*; InTech, 2016.

15. Cam, M. E.; Ertas, B.; Alenezi, H.; Hazar-Yavuz, A. N.; Cesur, S.; Ozcan, G. S.; Edirisinghe, M. Accelerated diabetic wound healing by topical application of combination oral antidiabetic agents-loaded nanofibrous scaffolds: An in vitro and in vivo evaluation study. Materials Science and Engineering: C **2020**, 111586. doi:10.1016/j.msec.2020.111586.

16. Samadian, H.; Zamiri, S.; Ehterami, A.; Farzamfar, S.; Vaez, A.; Khastar, H.; Salehi, M. Electrospun cellulose acetate/gelatin nanofibrous wound dressing containing berberine for

diabetic foot ulcer healing: in vitro and in vivo studies. Scientific Reports **2020**, 10(1). doi:10.1038/s41598-020-65268-7.

17. Koski, A.; Yim, K.; Shivkumar, S. Effect of Molecular Weight on Fibrous PVA Produced by Electrospinning. *Mater Lett* **2004**, *58*, 493–497, doi:10.1016/S0167-577X(03)00532-9.

18. Ulag, S., Ilhan, E., Demirhan, R., Sahin, A., Yilmaz, B. K., Aksu, B., Sengor, M., Ficai, D., Titu, A. M., Ficai, A., Gunduz, O. Propolis-based nanofiber patches to repair corneal microbial keratitis. *Molecules* **2021**, 26(9), 2577, doi: 10.3390/molecules26092577

19. Roncaglioni, M.C.; Reyers, I.; Cerletti, C.; Donati, M.B.; de Gaetano, G. Moderate Anticoagulation by Salicylate Prevents Thrombosis without Bleeding Complications. *Biochem Pharmacol* **1988**, *37*, 4743–4745, doi:10.1016/0006-2952(88)90346-2.

20. Zhang, X.; Tang, K.; Zheng, X. Electrospinning and Crosslinking of COL/PVA Nanofiber-Microsphere Containing Salicylic Acid for Drug Delivery. *J Bionic Eng* **2016**, *13*, 143–149, doi:10.1016/S1672-6529(14)60168-2.

21. Patel, D.M.; Patel, D.K.; Patel, C.N. Formulation and Evaluation of Floating Oral *In Situ* Gelling System of Amoxicillin. *ISRN Pharm* **2011**, *2011*, 1–8, doi:10.5402/2011/276250.

22. Wei, Q. *Functional Nanofibers and Their Applications*; 1st ed.; Woodhead Publishing, 2012.

23. Rosic. Romana; Kocbek, P.; Pelipenko, J.; Kristl, J.; Baumgartner, S. Nanofibers and Their Biomedical Use. *Acta Pharm* **2013**, *63*, 295–304.

24. Wu, L.; Yuan, X.; Sheng, J. Immobilization of Cellulase in Nanofibrous PVA Membranes by Electrospinning. *J Memb Sci* **2005**, *250*, 167–173, doi: 10.1016/j.memsci.2004.10.024.

25. Kharazmi, A.; Faraji, N.; Mat Hussin, R.; Saion, E.; Yunus, W.M.M.; Behzad, K. Structural, Optical, Opto-Thermal and Thermal Properties of ZnS–PVA Nanofluids Synthesized through a Radiolytic Approach. *Beilstein Journal of Nanotechnology* **2015**, *6*, 529–536, doi:10.3762/bjnano.6.55.

26. Sofokleous, P.; Stride, E.; Edirisinghe, M. Preparation, Characterization, and Release of Amoxicillin from Electrospun Fibrous Wound Dressing Patches. *Pharm Res* **2013**, *30*, 1926–1938, doi:10.1007/s11095-013-1035-2.

27. Thomas, D.; Zhuravlev, E.; Wurm, A.; Schick, C.; Cebe, P. Fundamental Thermal Properties of Polyvinyl Alcohol by Fast Scanning Calorimetry. *Polymer (Guildf)* **2018**, *137*, 145–155, doi: 10.1016/j.polymer.2018.01.004.

28. Pant, H.R.; Baek, W.; Nam, K.-T.; Jeong, I.-S.; Barakat, N.A.M.; Kim, H.Y. Effect of Lactic Acid on Polymer Crystallization Chain Conformation and Fiber Morphology in an Electrospun Nylon-6 Mat. *Polymer (Guildf)* **2011**, *52*, 4851–4856, doi: 10.1016/j.polymer.2011.08.059.

29. Rahimi Tanha, N.; Nouri, M. An Experimental Study on the Coaxial Electrospinning of Silk Fibroin/Poly(Vinyl Alcohol)–Salicylic Acid Core-Shell Nanofibers and Process Optimization Using Response Surface Methodology. *Journal of Industrial Textiles* **2018**, *48*, 884–903, doi:10.1177/1528083717747334.

30. Salman, S.A.; Bakr, N.A.; Homad, H.T. DSC and TGA Properties of PVA Films Filled with Na2S2O3.5H2O Salt. *J Chem Biol Phys Sci* **2018**, *8*, 001–011.

31. Ojah, N.; Saikia, D.; Gogoi, D.; Baishya, P.; Ahmed, G.A.; Ramteke, A.; Choudhury, A.J. Surface Modification of Core-Shell Silk/PVA Nanofibers by Oxygen Dielectric Barrier Discharge Plasma: Studies of Physico-Chemical Properties and Drug Release Behavior. *Appl Surf Sci* **2019**, *475*, 219–229, doi: 10.1016/j.apsusc.2018.12.270.

Table 1. Physical characterization results of the solutions.

Solutions	Density (g/cm^3)	Electrical conductivity (μS/cm)	Surface tension (mN/m)	Viscosity (mPa.s)
13wt.% PVA	1.038	706 ± 6.25	35.86 ± 1.2	9760
13wt.% PVA + AMX	1.087	646 ± 3	35.38 ± 1.38	7030
13wt.% PVA + SA	1.052	631.7 ± 5.7	37.74 ± 0.57	7875
13wt.% PVA + AMX + SA	1.048	609.3 ± 2.1	37.36 ± 0.66	7223

Table 2. The tensile test results of the nanofiber patches.

Fibers	Tensile strength (MPa)	Strain at break (%)
13wt.% PVA	4.31 ± 0.22	34.03 ± 9.55
13wt.% PVA + AMX	16.64 ± 2.12	51.58 ± 6.57
13wt.% PVA + SA	12.91 ± 1.54	58.89 ± 3.25
13wt.% PVA + AMX + SA	17.48 ± 3.27	57.29 ± 18.02

Table 3. The antimicrobial activity results of the nanofiber patches.

Fibers	*S. aureus* ATCC 29213 Inhibition zone (mm)	*E.coli* ATCC 25922 Inhibition zone (mm)
13wt.% PVA	0	0
13wt.% PVA+AMX	12	0
13wt.% PVA+SA	0	0
13wt.% PVA+AMX+SA	6	0
Ampicillin (10 µg)*	15	17

** Discs containing antibiotics used for positive control*

Figure Captions

Figure 1. The schematic representation of the nanofiber fabrication stages.

Figure 2. The FTIR spectrums of the drugs and nanofiber patches (A): 13wt.% PVA (A, a), AMX (A, b), SA (A, c), 13wt.% PVA+AMX (A, d), 13wt.% PVA+SA (A, e), and 13wt.% PVA+AMX+SA (A, f); The DSC thermographs of the pure drugs (B) and nanofiber patches (C): 13wt.% PVA (C, a), 13wt.% PVA+AMX (C, b), 13wt.% PVA+SA (C, c), and 13wt.% PVA+AMX+SA (C, d).

Figure 3. The SEM images of the 13wt.% PVA (a), 13wt.% PVA+AMX (b), 13wt.% PVA+SA (c), and 13wt.% PVA+AMX+SA (d) nanofiber patches before cross-linking.

Figure 4. The SEM images of the 13wt.% PVA (a), 13wt.% PVA+AMX (b), 13wt.% PVA+SA (c), and 13wt.% PVA+AMX+SA (d) nanofiber patches after cross-linking.

Figure 5. The drug release profiles of the AMX and SA from the 13wt.% PVA matrix. The calibration curve of the AMX (a), absorbance graph (c), and cumulative release graph of the AMX from the patches (e). The calibration curve of the SA (b), absorbance graph (d), and cumulative release graph of the SA from the patches (f).

Figure 6. The viability percentages of the fibroblast cells on the nanofiber patches (a) and fluorescence images of the cells on the nanofiber patches (b) after 1, 3, and 7 days of incubation.

Figure 7. The SEM images of the fibroblast cells on the nanofiber patches after fixation: 13wt.% PVA (a, b, c), 13wt.% PVA+AMX (d, e, f), 13wt.% PVA+SA (g, h, i), and 13wt.% PVA+AMX+SA (j, k, l).

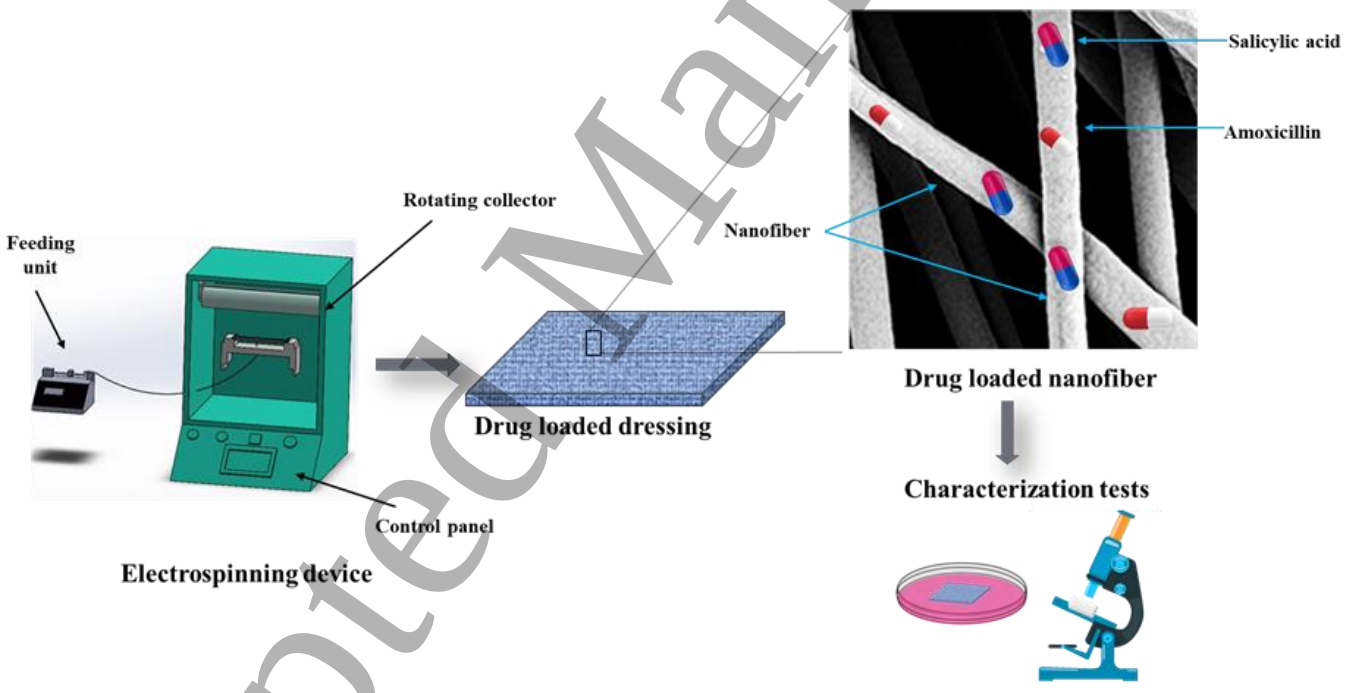

Figure 1.

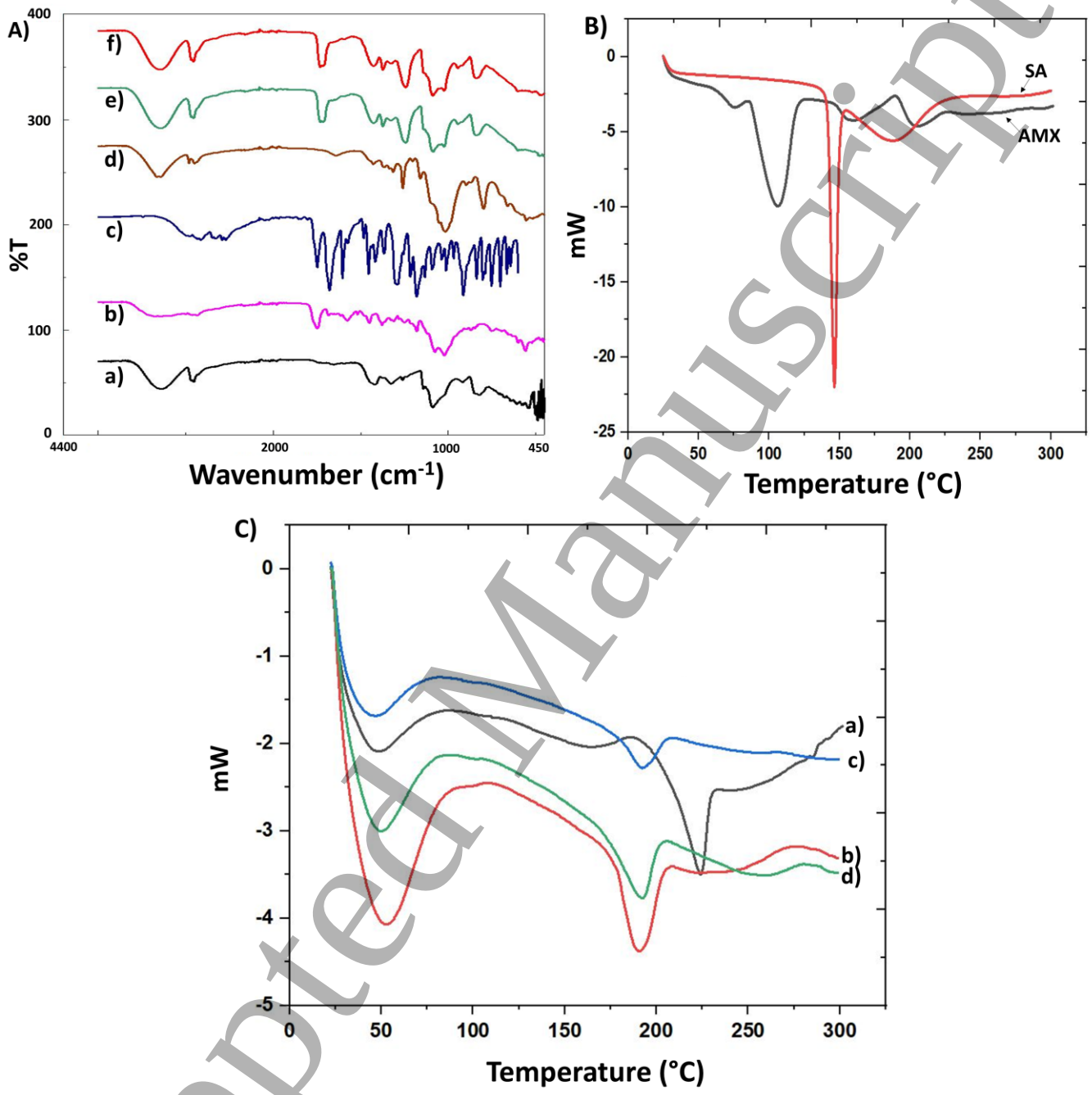

Figure 2.

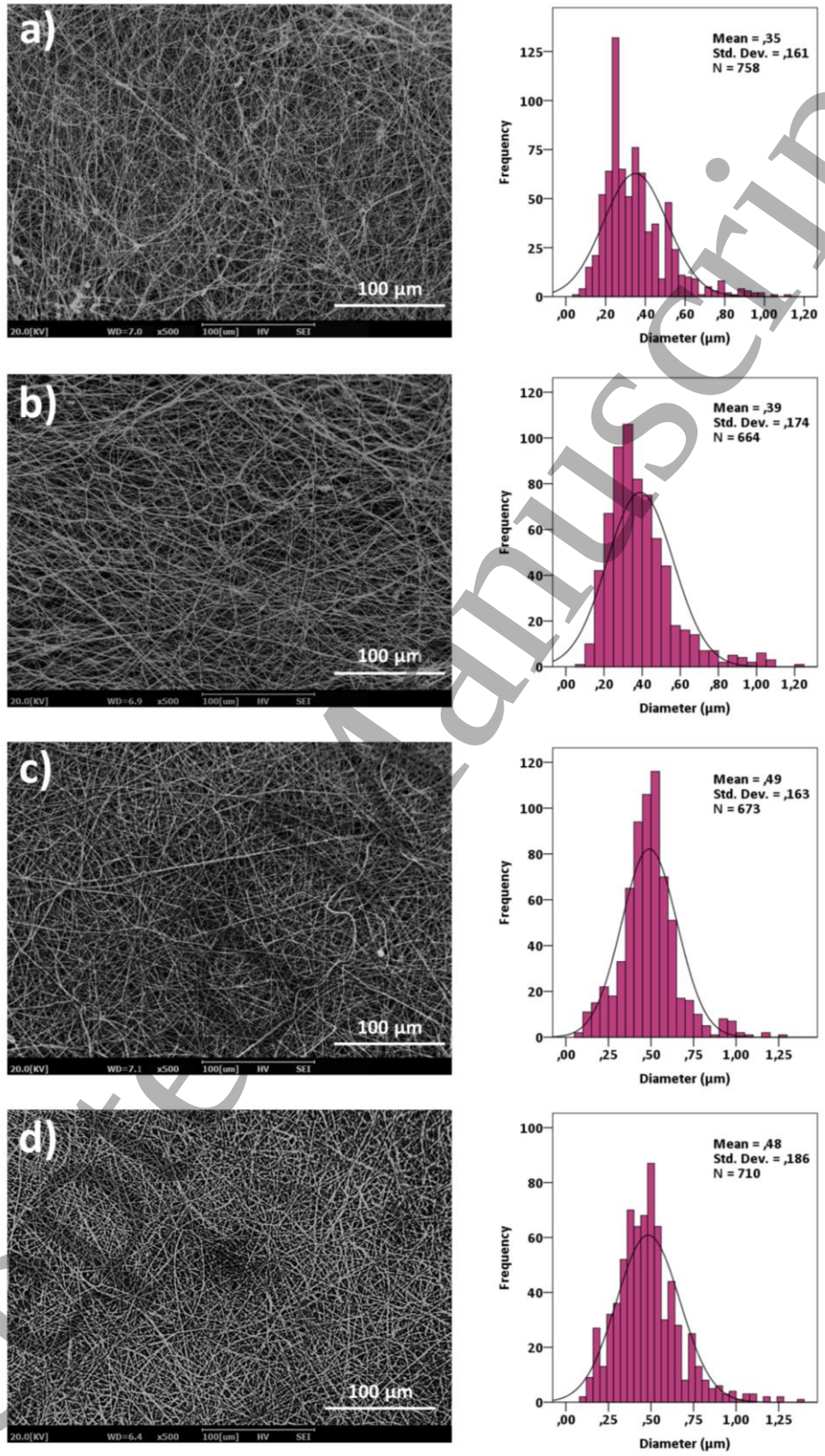

Figure 3.

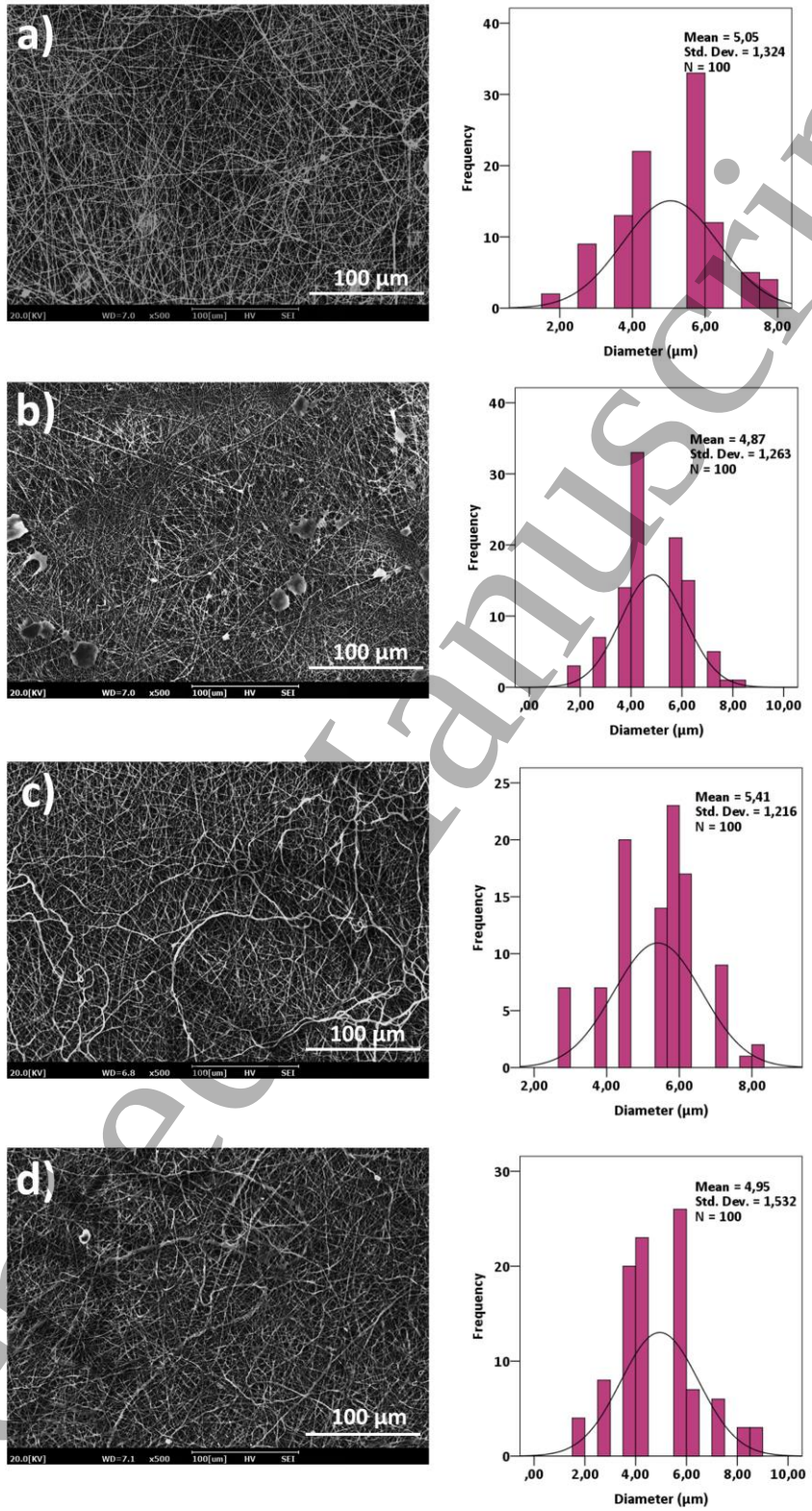

Figure 4.

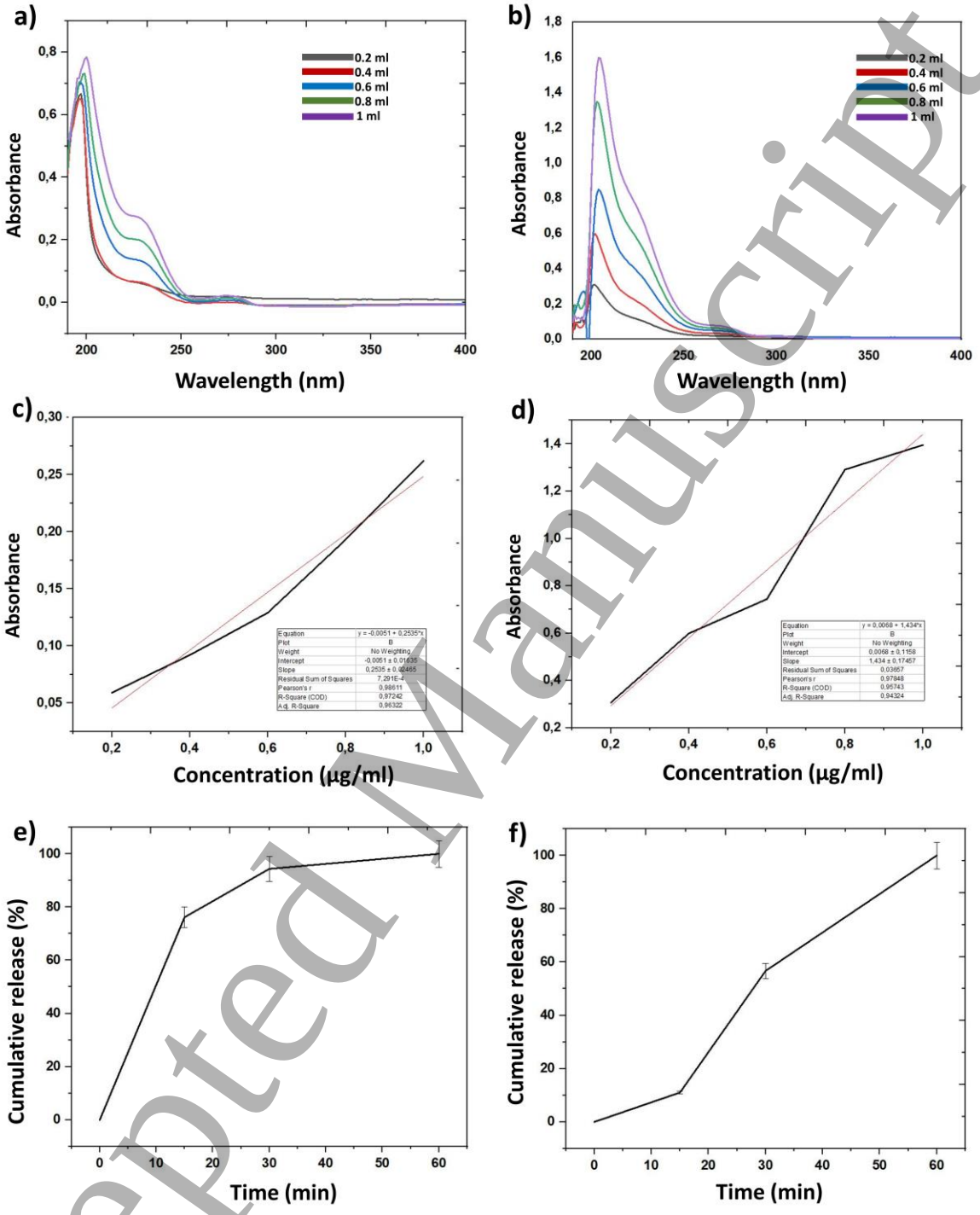

Figure 5.

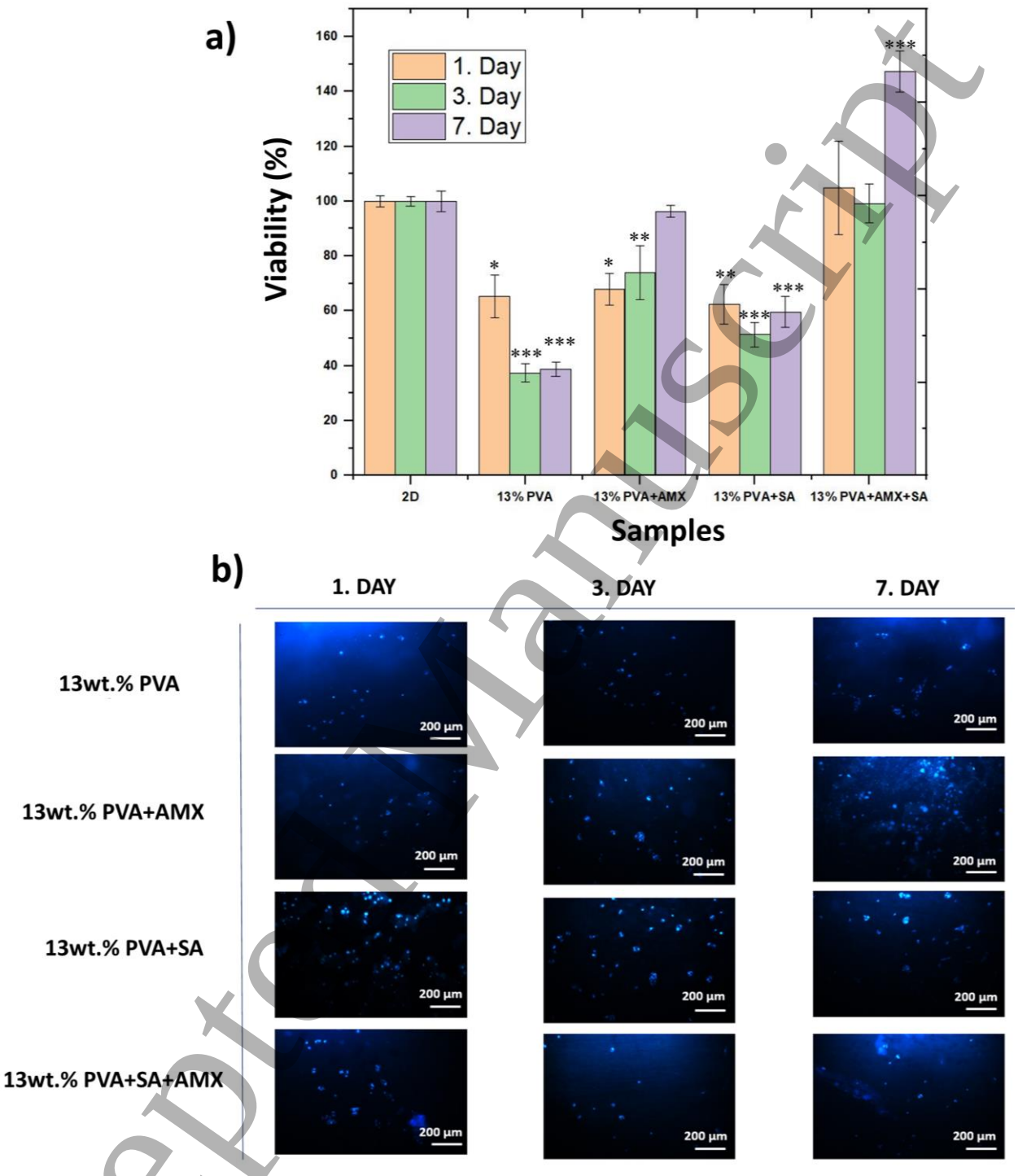

Figure 6.

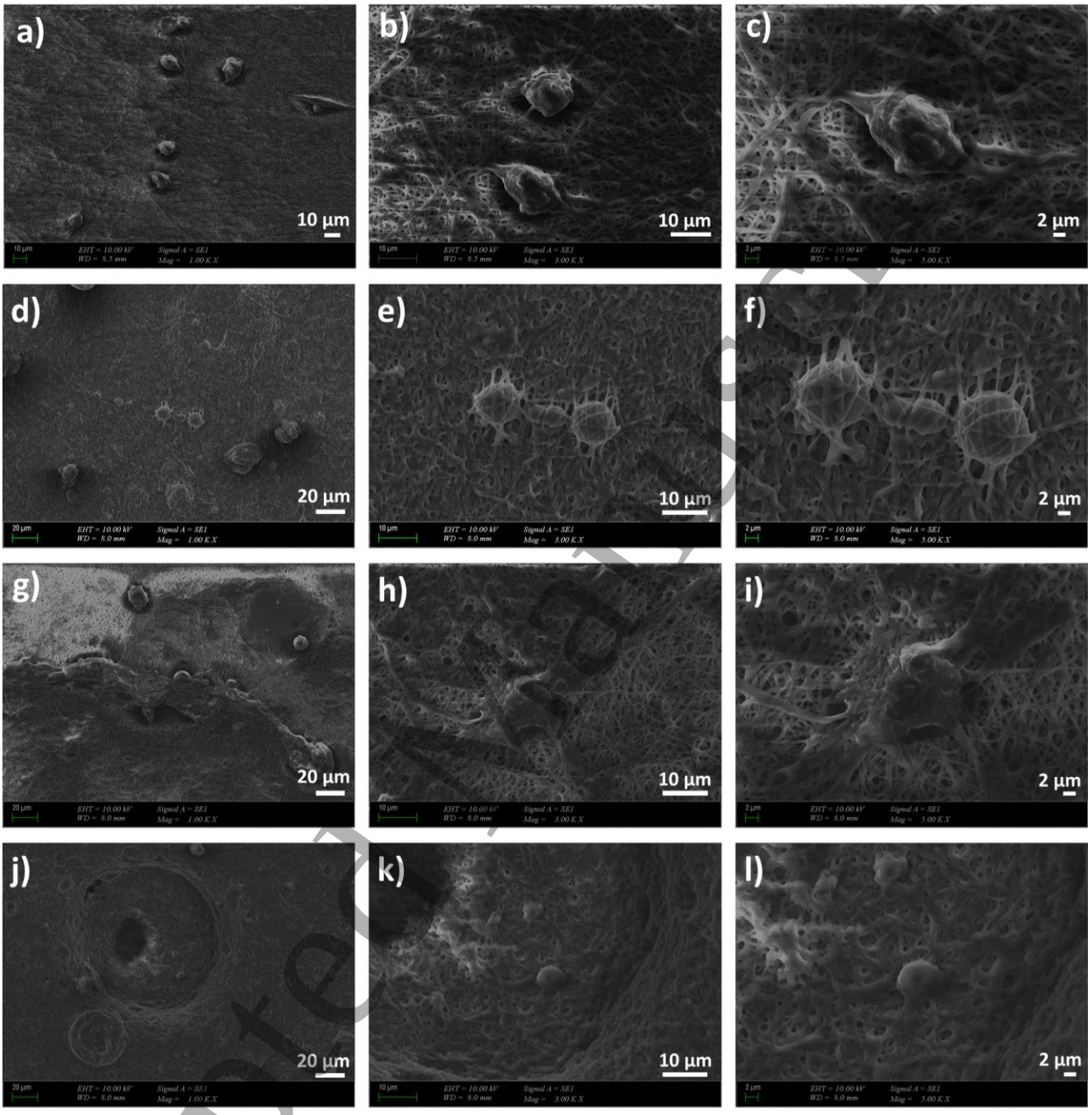

Figure 7.